Progress In Electromagnetics Research, Vol. 150, 197–203, 2015

An Omnidirectional Triple-Band Circular Patch Antenna Based on Open Elliptical-Ring Slots and the Shorting Vias

Wen-Feng Chen*, Dan Yu, and Shu-Xi Gong

Abstract—A circular patch antenna based on open elliptical-ring slots and shorting vias with conical radiation patterns is proposed. Fed by the coaxial probe at the center of the circular patch, the proposed antenna is excited at three resonant modes, simultaneously. The first resonant mode (monopolar patch mode) is achieved by six shorting vias, each of which is placed at the center of the open elliptical-ring slot. By embedding six open elliptical-ring slots on the patch, the other two resonant modes of the open elliptical-ring slot resonator, TE_{110} and TE_{210}, can also be excited. Due to symmetrical slots on the patch, these two modes can produce conical patterns, and their frequency ratio can also be tuned by adjusting the size of the slots. The proposed antenna is fabricated and measured. The measured results show that the proposed antenna can provide three operating bands which meet the required bandwidth specifications of 2.4/5.8 GHz WLAN and 3.5/5.5 GHz WiMAX standards. Detailed design considerations of the proposed antenna are described, and both the simulated and measured results are given. Moreover, the effects of the vital parameters on the performance of the proposed antenna are analyzed in this paper.

1. INTRODUCTION

With the rapid development of modern wireless communication systems, multiband antennas with simple structures have gained more attention than ever. Planar printed monopole and dipole antennas [1–6], especially with the multi-band characteristics, are promising candidates in wireless portable communication systems in virtue of their low profile, light weight, large service area and easy fabrication. To realize multiband operation, ultra-wideband (UWB) monopole antennas with band-notched characteristics by using meander lines [1] and arc-shaped stubs [2] are proposed. Differently, the multiband behavior has been obtained by extending the geometry of a reference shape adding T-shaped strips [3, 4], Y-shaped stubs [5] or mirrored-L elements [6]. Most of the monopole antennas have partial ground plane. However, their impedance and radiation characteristics are significantly influenced by the size of the ground plane.

Recently, some low profile microstrip antennas with intact ground plane have been reported in [7–9]. For example, by embedding an offset open-ring slot [8] or two open-ring slots [9] in a circular patch, two resonant modes with similar radiation patterns are excited. However, these antennas radiate broadside patterns and cannot be widely used in the wireless communications. To realize the monopole-like radiation pattern, some microstrip patch antennas with low profile have been investigated in [10–12]. In [10], a conical radiation pattern is obtained by using a circular patch antenna (CPA). Then, an annular ring was utilized to improve the impedance bandwidth of the CPA [11]. Finally, a shorted square-ring fed by a top-loaded coaxial probe is studied in [12], where the shorting vias are added to excite the monopolar patch mode and change the frequency ratio of the resonant frequencies.

In this paper, a triple-band center-fed circular microstrip antenna loaded with shorting vias and open elliptical-ring slots is introduced for WLAN and WiMAX applications. The shorting vias enclosed

Received 2 January 2015, Accepted 11 February 2015, Scheduled 4 March 2015
* Corresponding author: Wen-Feng Chen (347614321@qq.com).
The authors are with the Science and Technology on Antenna and Microwave Laboratory, Xidian University, Xi'an 710071, P. R. China.

by the open elliptical-ring slots are located symmetrically with respect to the central coaxial probe. Furthermore, the ground plane is intact which makes the proposed antenna a low profile configuration of $0.048\lambda_0$ at 2.4 GHz. Due to the central feeding by the coaxial probe, the proposed antenna provides good omnidirectional radiation patterns and the low gain variation in the azimuth plane across the three resonant bands. Both simulation and measurement results are presented to validate the antenna performance.

2. THEORY AND ANTENNA CONFIGURATION

2.1. Resonant Mode Analysis of the Open Elliptical-Ring Slot

It is well known that any slot has its complementary form in wires or strips, thus, patterns and impedances data of these forms can be used to predict the patterns and impedances of corresponding slots. The electric field distributions of microstrip open-ring resonator's resonant modes are given in [13]. Combining with the electric field distributions of the microstrip elliptical ring resonator's resonant modes in [14], the electric field distributions of the open elliptical-ring slot resonator's TM_{110} and TM_{210} modes, which are shown in Figure 1, can be reduced with the Babinet's principle. According to duality principle, there is an interchange between the electromagnetic fields of the slot and the complementary ring which is also presented in Figure 1.

The resonant frequencies of both the TM_{110} and TM_{210} modes can be estimated by the microstrip line resonator analysis method which is used in [13]. The TM_{110} mode is the one with the lowest resonant frequency, as shown in Figure 2(a). And it can be considered as the resonance on a curved $\lambda/2$ microstrip line. The distribution of the magnetic field strength far away from the gap is nearly equal to that of a straight microstrip line. Only in the gap area does the field distribution change, because the field must be perpendicular to the boundaries at the end of the lines. The electric field component E_Z is nearly constant across the microstrip line and only changes slightly from the inner to the outer circumference. For TM_{210} mode, an additional zero of the azimuthal component H_ϕ is found, and the corresponding field distribution is shown in Figure 2(b). The mean value of the resonator length now is nearly equal to one wavelength. The resonance characteristics of the proposed antenna and the effects of key parameters are performed in the following section.

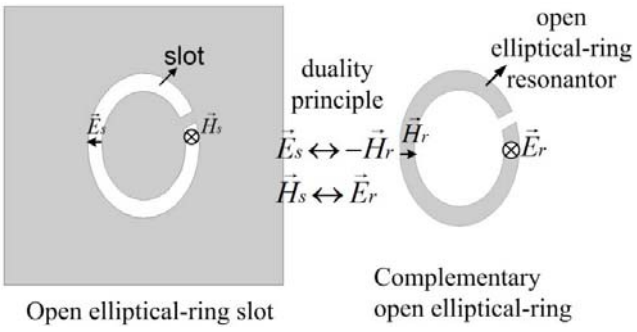

Figure 1. Open elliptical-ring slot resonator and the complementary open elliptical-ring resonator.

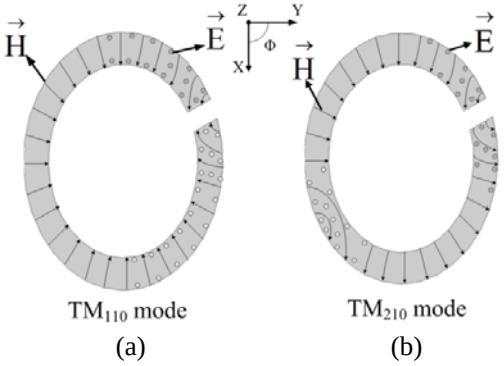

Figure 2. Distributions of the electromagnetic field of the TM_{110} and TM_{210} modes.

2.2. Antenna Design Procedure

Figure 3 presents the geometry of the proposed antenna. The circular patch with radius r_2 is printed on a substrate of thickness $h = 6$ mm, relative permittivity 2.65 and loss tangent 0.0025. And both the substrate and ground plane have radius r_1. Six shorting vias of radius r_4 are uniformly distributed along a circle with a displacement of r_3 from the feeding point. Then, six open elliptical-ring slots are embedded to enclose each of the shorting vias. The details of the open elliptical-ring slots are shown in Figure 3(b). The open elliptical-ring slot has an inner semi-minor axis of a_1 and an inner semi-major

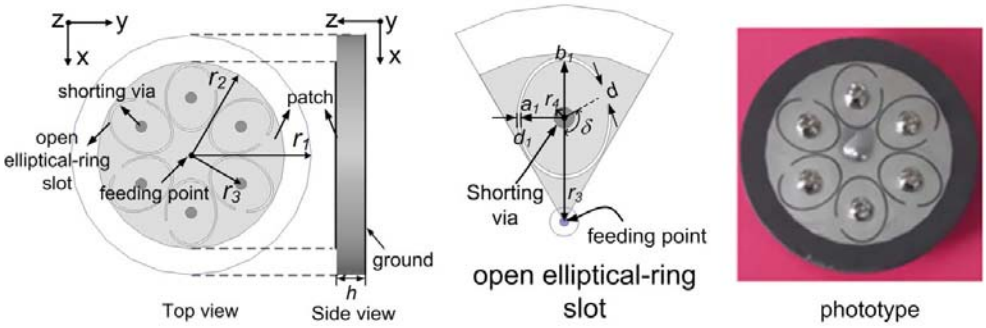

Figure 3. Geometry and photograph of the proposed antenna with the sizes of $r_1 = 30\,\text{mm}$, $r_2 = 23.4\,\text{mm}$, $r_3 = 14.4\,\text{mm}$, $r_4 = 1.5\,\text{mm}$, $a_1 = 6.1\,\text{mm}$, $b_1 = 7.93\,\text{mm}$, $h = 6\,\text{mm}$, $d_1 = 3\,\text{mm}$, $d_2 = 0.4\,\text{mm}$, and $\delta = 120°$. (a) Top and side view of the proposed antenna. (b) The details of the open elliptical-ring slot. (c) Photograph of the proposed antenna.

axis of b_1 with width d_1. However, the ratios between the major and minor axes of both the outer and inner ellipses are equal to b_1/a_1. The gap between the two open ends of each open elliptical-ring slot is d, and the angle between the gap center and major axis is δ. For providing good radiation pattern performances across the three bands, the coaxial probe is placed at the center of the patch with the probe radius of 0.6 mm.

3. PARAMETRIC STUDY

The effects of vital parameters of the proposed antenna on the resonant frequency and impedance matching are discussed in this section.

3.1. Effects of Variation of the Slot Gap *d*

Figure 4 shows $|S_{11}|$ of the proposed antenna for different values of slot gap d. The other parameters of the antenna are shown in the caption of Figure 3. It is observed that when d increases, the second resonant frequency (TE_{110} mode of the open elliptical-ring slot) increases for the decrease of the resonance path of the open elliptical-ring. Also, the increase of gap d causes a poor impedance matching at the third resonant frequency (TE_{210} mode of the open elliptical-ring slot). From Figure 4, it can be seen that the first resonant frequency (monopolar patch mode) changes slightly since the position of the shorting vias does not change.

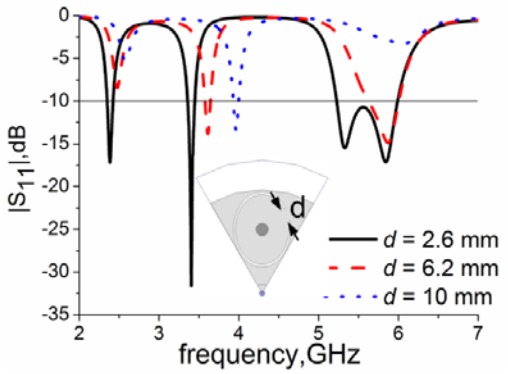

Figure 4. The simulated reflection coefficients with different sizes of gap d.

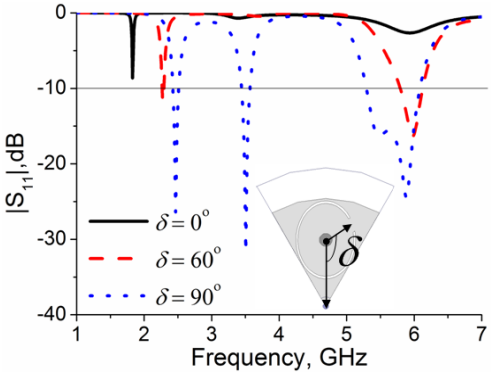

Figure 5. The simulated reflection coefficients with different angles δ of the gap.

3.2. Effects of Variation of the Angle δ

$|S_{11}|$ of the proposed antenna with different values of angle δ is shown in Figure 5 with other parameters shown in the caption of Figure 3. It can be noticed from the figure that as the value of δ decreases, the first resonant frequency decreases, and there is only slight change in the second and third resonant frequencies. However, the decrease of δ, which means that the feeding position of the open elliptical-ring slot is changed, causes a poor impedance matching at the second and third resonant frequencies.

3.3. Effects of Variation of a_1

Figure 6 shows $|S_{11}|$ of the proposed antenna for different values of a_1 (or slot width d_1) with the other parameters shown in the caption of Figure 3. It is observed that when the value of a_1 increases (or slot width of d_1 decreases), the second and third resonant frequencies decrease due to the increase of the mean resonance path of the open elliptical-ring slot. Also, impedance matching of the second and third resonant frequencies turns better with the decrease of slot width. However, the first resonant frequency, dependent on the angle δ and the position of the shorting vias, changes little.

3.4. Effects of Variation of the Distances between Two Adjacent Slots

Figure 7 shows $|S_{11}|$ of the proposed antenna for different distances between two adjacent slots with the other parameters shown in the caption of Figure 3. Noting that the slot width and the ratio between major and minor axes (b_1/a_1) are fixed when changing the distance between two adjacent slots. It is easily found that when the distance between two adjacent slots increases (the size of the slot decreases), the second and third resonant frequencies turn impedance mismatching for the weak coupling between the slots, but there is no change in the first resonant frequency. Therefore, the number of slots should be properly chosen in order to get a good impedance matching at both the TE_{110} and TE_{210} modes of the open elliptical-ring slot. In this paper, considering the radius of the circular patch, the number of slots is six.

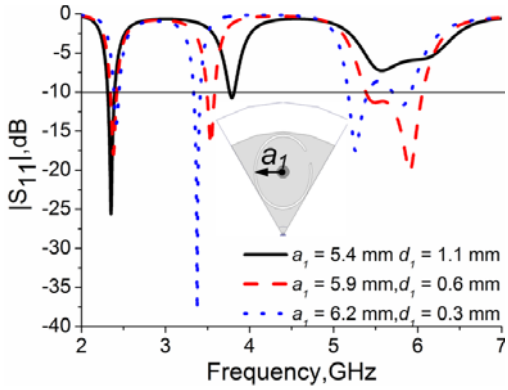

Figure 6. The simulated reflection coefficients with different values of a_1 and d_1.

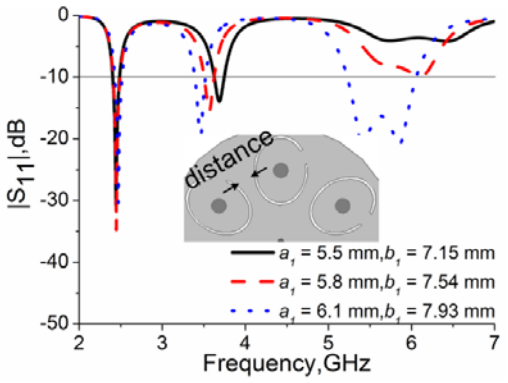

Figure 7. The simulated reflection coefficients with different distances between the slots.

3.5. Effects of Variation of the Ratios between Major and Minor Axes

Figure 8 shows $|S_{11}|$ of the proposed antenna for different ratios between major and minor axes. The other parameters of the antenna are fixed as shown in the caption of Figure 3. The shorting via position of r_3 is accordingly adjusted to maintain the adjacent slots not to overlap while the slot width is fixed. It is easily found that as the ratio between major and minor axes increases, the second and third resonant frequencies increase, and there is no change in the first resonant frequency. Also, the increased ratio makes the impedance matching of the whole resonant frequencies good and the two resonant frequencies of the TE_{210} mode couple together to form the third resonant band. When the ratio is equal to 1, the open elliptical-ring slot becomes an open-ring slot, and a poor impedance matching is

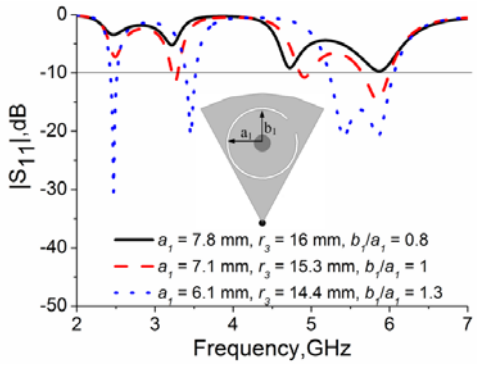

Figure 8. The simulated reflection coefficients with different ratios between major and minor axes.

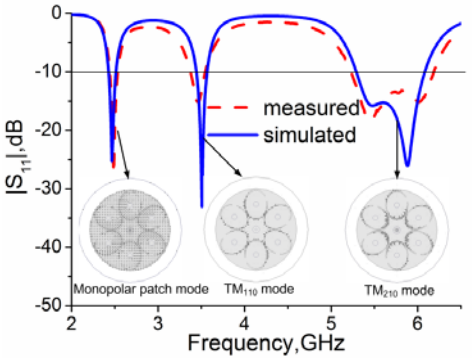

Figure 9. The experimental and simulated $|S_{11}|$ of the proposed antenna.

obtained. Therefore, an open elliptical-ring slot, not an open-ring slot, is necessary for the design of the proposed triple-band circular patch antenna.

4. RESULTS AND DISCUSSIONS

To verify the theory, a prototype, shown in Figure 3(c), is fabricated and measured. The measured and simulated $|S_{11}|$ of the prototype are presented in Figure 9, and a good agreement is achieved except for an acceptable frequency discrepancy which may be caused by the fabrication error. From the measured results in Figure 9, it is clearly observed that three resonant modes are excited, and their resonant frequencies (defined as the frequencies with minimum $|S_{11}|$) are about 2.4 GHz, 3.5 GHz, 5.5 GHz and 6.0 GHz, which belong to the monopolar patch mode, TE_{110} and TE_{210} modes, respectively. It should be mentioned that both the third and fourth operating frequencies, which are belong to the even and the odd modes for the TE_{210} mode [14] of the open elliptical-ring slots, are dependent on gap d and angle δ. The impedance bandwidths of the first and second operating frequencies are 3.7% (2.39–2.48 GHz) and 5.8% (3.33–3.53 GHz), respectively. The third and fourth operating frequencies are coupled together with impedance bandwidths of 17.5% (5.2–6.2 GHz). Therefore, the proposed antenna can provide operating bands covering 2.4/5.8 GHz WLAN and 3.5/5.5 GHz WiMAX successfully.

Figure 9 also shows the simulated electric field distributions of the proposed antenna at the three resonant frequencies. At 2.4 GHz, the electric field distributions of monopolar patch mode assuredly similar to the top-loaded monopole are invariable in the Φ-direction, and their directions are along the radial direction of the patch with only Z-component, so that the monopolar patch mode gives a null in the broadside. For the TE_{110} and TE_{210} modes, the electric field distributions on the open elliptical-ring slots agree well with the magnetic field distributions on the complementary open elliptical-ring which is shown in Figure 2.

For the radiation patterns test of the prototype, we have used a standard antenna test set with a horn antenna as a source in an anechoic chamber. Simulated and measured co-polarization (E_θ) and cross-polarization (E_φ) radiation patterns on E-plane and H-plane are exhibited in Figure 10 at different resonant frequencies, with the x-z plane and x-y plane referred to as the E- and H-planes, respectively. The results show that the proposed antenna radiates stable vertical-polarized waves (E_θ) with conical radiation patterns across the whole operating bandwidths, and the maximum power levels occur at elevation angle θ of 81°, 66°, 39° and 33° as it is operated at 2.4, 3.5, 5.5, and 5.8 GHz, respectively, which are similar to the simulation results by HFSS.

Finally, the measured gain variations against frequency for various elevation angles θ across three operating bands are measured and shown in Figure 11. As can be found, the elevation angle θ, at which the maximum power level occurs, decreases with the increase of the frequency. For the case of $\theta = 60°$, the average gains are about 1.285 dBi (1.27–1.3 dBi) with variation of 0.03 dBi at the 2.4 GHz band, 1.11 dBi (1.09–1.13 dBi) with variation of 0.04 dBi at the 3.5 GHz band, 2.39 dBi (1.67–3.12 dBi) with variation of 1.45 dBi at the 5.5 and 5.8 GHz bands.

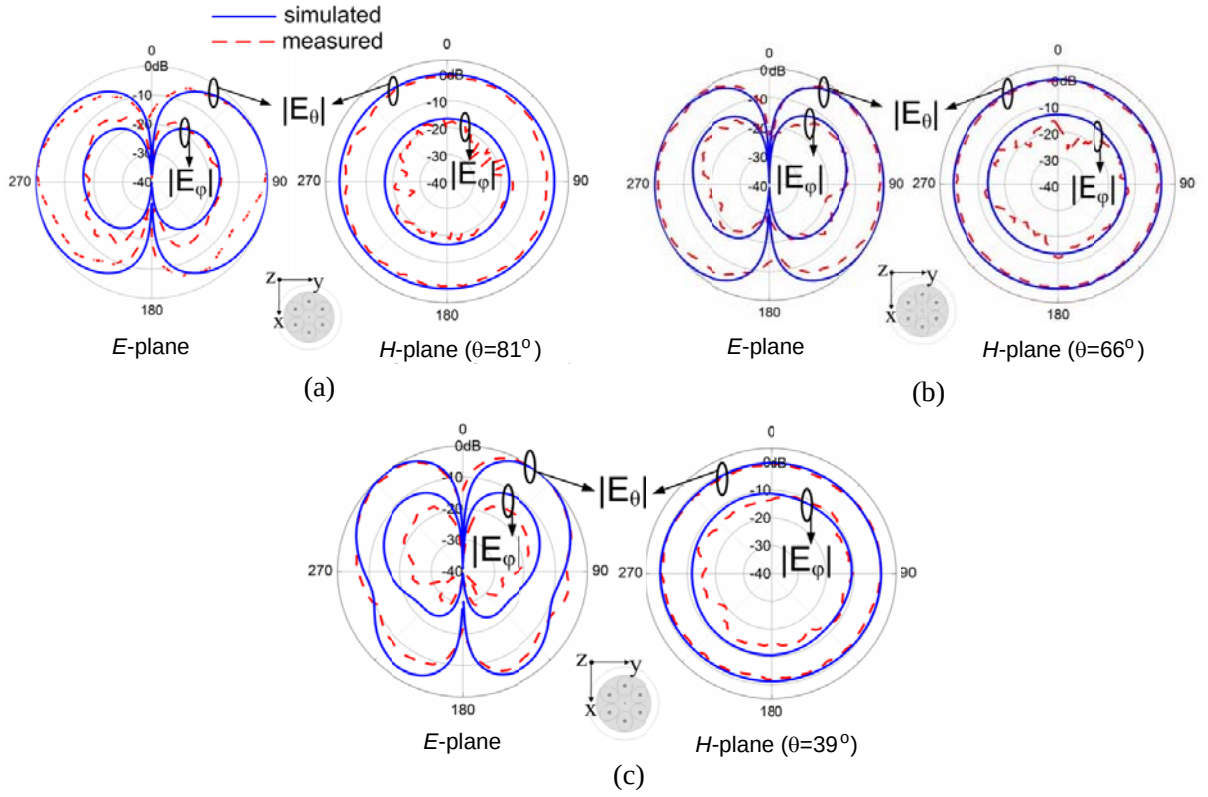

Figure 10. The measured and simulated radiation patterns of the prototype at different resonant frequencies. (a) At 2.4 GHz. (b) At 3.5 GHz. (c) At 5.5 GHz. (d) At 5.8 GHz.

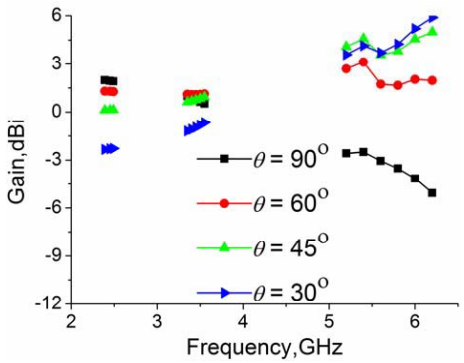

Figure 11. Measured gain variations against frequency for various θ across 2.5, 3.5, 5.5 and 5.8 GHz operating bands.

5. CONCLUSION

A triple-band center-fed circular microstrip antenna loaded with shorting vias and embedded with open elliptical-ring slots is proposed. The proposed antenna has an attractive low-profile configuration with a 6 mm height only ($0.048\lambda_0$ at 2.4 GHz). Three resonant modes with conical radiation patterns can be excited by feeding symmetrically at the center, and the key parameters which affect the resonant frequencies of the three modes are also studied. An antenna prototype is designed, fabricated, and tested. The experimental results show that the impedance bandwidths of the three operating frequencies are 3.7%, 5.7%, and 17.5%, respectively. Also, the antenna can provide stable conical radiation patterns across these three operating bands. Therefore, the proposed design is suitable for the applications of the present wireless communications.

REFERENCES

1. Weng, Y. F., S. W. Cheung, and T. I. Yuk, "Design of multiple band-notch using meander lines for compact ultra-wide band antennas," *IET Microw. Antennas Propag.*, Vol. 6, No. 8, 908–914, 2012.
2. Moghaddasi, M. N., A. Danideh, R. Sadeghifakhr, and M. R. Azadi, "CPW-fed ultra wideband slot antenna with arc-shaped stub," *IET Microw. Antennas Propag.*, Vol. 3, No. 4, 681–686, 2009.
3. Luo, Y. L. and K. L. Wong, "Printed double-T monopole antenna for 2.4/5.2 GHz dual-band WLAN operations," *IEEE Trans. Antennas Propag.*, Vol. 51, No. 9, 2187–2192, 2003.
4. Chang, T. N. and J. H. Jiang, "Meandered T-shaped monopole antenna," *IEEE Trans. Antennas Propag.*, Vol. 57, No. 12, 3976–3978, 2009.
5. Liu, W.-C. and C.-F. Hsu, "Dual-band CPW-fed Y-shaped monopole antenna for PCS/WLAN application," *Electron. Lett.*, Vol. 41, No. 7, 390–391, 2005.
6. Chaimool, S. and K.-L. Chung, "CPW-fed mirrored-L monopole antenna with distinct triple bands for WiFi and WiMAX applications," *Electron. Lett.*, Vol. 45, No. 18, 928–929, 2009.
7. Lee, S. Y. and C. C. Yu, "A novel wideband asymmetric hybrid antenna for WLAN/WiMAX applications," *Microw. Opt. Technol. Lett.*, Vol. 51, No. 4, 1055–1057, 2009.
8. Jan, J.-Y., "Single-layer single-feed dual-frequency circular microstrip antenna with an offset open-ring slot," *IEEE Trans. Antennas Propag.*, Vol. 51, No. 10, 3010–3012, 2003.
9. Jan, J.-Y. and K.-L. Won, "A broadband circular microstrip antenna two open-ring slots," *Microw. Opt. Technol. Lett.*, Vol. 23, No. 4, 205–207, 1999.
10. Economou, L. and R. J. Langley, "Patch antenna equivalent to simple monopole," *Electron. Lett.*, Vol. 33, No. 9, 727–729, 1997.
11. Al-Zoubi, A., F. Yang, and A. Kishk, "A broadband center-fed circular patch-ring antenna with a monopole like radiation pattern," *IEEE Trans. Antennas Propag.*, Vol. 57, No. 3, 789–792, 2009.
12. Lin, S.-J. and J.-S. Row, "Monopolar patch antenna with dual-band and wideband operations," *IEEE Trans. Antennas Propag.*, Vol. 56, No. 3, 900–903, 2008.
13. Wolff, I. and V. K. Tripathi, "The microstrip open-ring resonator," *IEEE Trans. Microwave Theory Tech.*, Vol. 32, No. 1, 102–107, 1984.
14. Kraus, J. D. and R. J. Marhefka, *Antennas: For All Applications,* 3rd Edition, Publishing House of Electronics Industry, Beijing, 2008.